Food Chemistry: X 15 (2022) 100420

Contents lists available at ScienceDirect

Food Chemistry: X

journal homepage: www.sciencedirect.com/journal/food-chemistry-x

Acylating blueberry anthocyanins with fatty acids: Improvement of their lipid solubility and antioxidant activities

Pengkai Wang [a,b], Jingna Liu [c], Yuanhong Zhuang [c], Peng Fei [c,*]

[a] College of Food Science and Technology, Guangdong Ocean University, Guangdong Provincial Key Laboratory of Aquatic Product Processing and Safety, Guangdong Provincial Engineering Technology Research Center of Seafood, Guangdong Province Engineering Laboratory for Marine Biological Products, Key Laboratory of Advanced Processing of Aquatic Product of Guangdong Higher Education Institution, Zhanjiang 524088, China
[b] Collaborative Innovation Center of Seafood Deep Processing, Dalian Polytechnic University, Dalian 116034, China
[c] School of Biological Science and Biotechnology, Minnan Normal University, Zhangzhou 363000, China

ARTICLE INFO

Keywords:
Anthocyanins
Fatty acids
Lipid solubility
Antioxidation activities
Density functional theory
Caenorhabditis elegans

ABSTRACT

Aimed at exploring the impact of fatty acid side chains on the anthocyanins, *n*-valeric acid, *n*-decanoic acid and myristic acid were used to grafting onto the blueberry anthocyanins, and the acylating degree value of the of *n*-valeric acid acylated anthocyanins (Va-An), *n*-decanoic acid acylated anthocyanins (De-An) and myristic acid acylated anthocyanins (My-An) reached 6.43 %, 7.56% and 8.38 %, respectively. After acylation modification, the octanol–water partition coefficient of the anthocyanins increased from −0.20 (native anthocyanins, Na-An) to 0.65 (Va-An), 0.66 (De-An) and 0.72 (My-An), respectively, indicating the increasement of the lipid solubility. Besides, although the DPPH clearance of acylated anthocyanins was lower than that of native anthocyanins, the inhibition ratio of β-carotene bleaching and malonaldehyde reduction effect of the acylated blueberry anthocyanins in *Caenorhabditis elegans* were both stronger than that of native anthocyanins, which might be caused by the improvement of lipid solubility of the anthocyanins.

1. Introduction

Anthocyanins, a kind of flavonoid substance formed by using 2-phenylbenzopyranoid cation as the parent nucleus and combining one or more sugar groups, are water-soluble pigments widely found in plants (Chandra Singh, Kelso, Price, & Probst, 2020; Chen et al., 2022; Oliveira Filho et al., 2021). So far, more than 600 anthocyanins have been isolated and identified from nature, mainly derived from 6 anthocyanidins, namely, cyanidin (Cy), delphinidin (De), pelargonidin (Pg), peonidin (Pn), petunidin (Pt) and malvidin (Ma), which account for more than 95 % of all anthocyanins (Fei et al., 2021; Zhao et al., 2017). In addition to making leaves, flowers, stems and fruits appear colorful, anthocyanins, with unpaired electrons, are hydrogen donors and can effectively eliminate a variety of reactive oxygen radicals (José Aliaño González, Carrera, Barbero, & Palma, 2022; Stoica et al., 2022; Zeng et al., 2019). A large number of studies have shown that anthocyanins have a wide range of pharmacological effects, such as promoting retinoid regeneration, anti-inflammatory, enhancing immunity, antioxidant, anti-aging, anti-tumor and other physiological activities (Grobelna et al., 2019a, 2019b; He & Giusti, 2010; Kalisz & Kieliszek, 2021; Kalisz et al., 2020). They are often used as a natural water-soluble pigment in food, medicine, feed additives and related fields. However, anthocyanins have high hydrophilicity due to their rich phenolic hydroxyl, which limits their application in fatty foods. On the other hand, poor lipid solubility also makes it difficult for anthocyanins to exert their antioxidant and related biological activities in fatty foods and even organisms (José Aliaño González et al., 2022). An effective way to improve their lipid solubility is introducing lipophilic groups into anthocyanins.

In this paper, aliphatic acyl chlorides were used to the acylated anthocyanins, and the effects of fatty acid side chains on the lipid solubility and antioxidant of anthocyanins were investigated, so as to provide theoretical basis for the expansion and application of anthocyanins in the field of expand its use in ice cream, sausages, grease, meat products and other fields.

2. Experiment

2.1. Materials and reagents

Blueberry anthocyanins extract (368.4 mg/g anthocyanin, measured

* Corresponding author.
E-mail address: fp@bio.mnnu.edu.cn (P. Fei).

https://doi.org/10.1016/j.fochx.2022.100420
Received 6 June 2022; Received in revised form 3 August 2022; Accepted 5 August 2022
Available online 8 August 2022

in Cyanidin-3-O-glucoside) was supplied by Xi'an Shengqing Biotechnology Co., ltd. (Xi'an, China). Before use, blueberry anthocyanins were dissolved in water, freeze-dried and powder collected; *n*-valeryl chloride, *n*-decanoyl chloride, myristyl chloride, *n*-octyl alcohol and 4-dimethylaminopyridine were purchased from Shanghai Aladdin Reagent Co., ltd. (Shanghai, China); Linoleic acid and 5-fluoro-20-deoxyuridine (FUdR) were obtained from Shanghai Macklin Biochemical Technology Co., ltd. (Shanghai, China); 1,1-diphenyl-2-picryl hydrazine (DPPH) was supplied by Shanghai Yuanye Biotechnology Co., ltd; Sodium hydroxide, hydrochloric acid, citric acid, absolute ethyl alcohol, Tween 80 and ethyl acetate were all analytically pure and purchased from Sinopharm Chemical Reagent Co., ltd. (Shanghai, China). *Caenorhabditis elegans* wild-type N2 was provided by Caenorhabditis Genetics Center of the University of Minnesota (Minneapolis, MN, USA). Uracil defective *Escherichia coli* OP50 and nematode growth medium (NGM) were obtained from Nanjing Jiancheng Bioengineering Co., ltd (Suzhou, China). Kits for superoxide dismutase (SOD) and malondialdehyde (MDA) were obtained from Suzhou Komin Biotechnology Co., ltd (Suzhou, China). All reagents used in this study were of analytical grade unless otherwise stated.

2.2. Apparatus

The functional groups of anthocyanins were characterized by a NICOLET IS 10 Fourier transform infrared spectrometer (FTIR, Thermo Fisher co., ltd, America). The scanning wavelength was 16 cm^{-1}, the scanning range was 4000^{-1}–400 cm^{-1}, and the scanning number was 64. The absorbance of anthocyanins in the ultraviolet and visible region was measured by a MultiSkan Go microplate reader (Thermo Fisher co., ltd, America). X-ray photoelectron spectroscopy (XPS, EscaLab 250Xi, Thermo Fisher co., ltd, America) is necessary to determine the surface element energy of anthocyanin. The wide scanning can be of 100 eV, with the resolution of 1.0 eV, while the fine scanning can be of 50 eV, with the resolution of 0.1 eV. Chemical shifts referred to the residual solvent signal of tetramethylsilane at δ_H 3.35 ppm (CD3OD).

2.3. Preparation of the acylated blueberry anthocyanins

2.3.1. Purification of blueberry anthocyanins extract

The blueberry anthocyanin extract was dissolved in absolute ethanol and then filtered through a microporous membrane (22 μm). Then, the filtrate obtained from the previous step was freeze-dried and the powder was collected. The powder was then added to acetone and stirred thoroughly before being filtered again. Finally, the solvent in the filter residue was removed by freeze-drying to obtain native anthocyanins (Na-An).

The anthocyanins content in blueberry anthocyanins extract was 368.4 mg/g (measured in Cyanidin-3-O-glucoside), which was measured through pH-differential method according to previous study (Liu et al., 2020). After purification, the content reached to 786.9 mg/g.

2.3.2. Preparation of the acylated blueberry anthocyanins

The acylated blueberry anthocyanins were prepared through solid states reaction method. Briefly speaking, 5 g the native blueberry anthocyanin and 30 mmol acyl donors (3.62 g *n*-valeryl chloride or 5.72 g *n*-decanoyl chloride or 7.40 g myristyl chloride) were added to the 50 mL polytetrafluoroethylene reactor, and 0.5 g 4-dimethylaminopyridine was added as the catalyst. After evenly stirring, the reactor was placed in an oven at 50 °C for 12 h to complete the acylation grafting reaction. The mixture was then cleaned with tetrahydrofuran and filtered to remove the 4-dimethylaminopyridine, unreacted acyl chloride and free fatty acids. The cleaning and filtering process were repeated three times. At last, the reaction products were vacuum dried at 50 °C for 3 h to remove residual tetrahydrofuran.

The native blueberry anthocyanin was coded as Na-An. The blueberry anthocyanins the acylated with *n*-valeric acid, *n*-decanoic acid and myristic acid were coded as Va-An, De-An and My-An, respectively.

2.4. Determination of the yield and the acylation degree (AD) of the acylated blueberry anthocyanins

2.4.1. Determination of the yield

The yield of the acylated anthocyanins was calculated based on Eq. (1):

$$Yield = \frac{m_1}{m_0} \times 100\% \quad (1)$$

where m_0 means the mass of the native anthocyanins used for modification; m_1 is the mass of the acylated anthocyanins.

The yield of Va-An, De-An and My-An, having done the calculation, were 87.69 %, 91.56 % and 88.57 %, respectively.

2.4.2. Determination of the AD value

Potentiometric titration was used to determine the esterification degree of the acylated anthocyanins, and it was slightly modified according to the method of Pinheiro et al (Pinheiro et al., 2008). First, 0.2 g of the acylated anthocyanin was dissolved in 20 mL (V_0) of 0.1 mol/L (C_0) sodium hydroxide solution, which was hydrolyzed and saponified by magnetic agitation for 2 h at 50 °C. Then add 0.01 mol/L (C_1) of hydrochloric acid to the mixture until the pH value is 9.0, and the volume of the hydrochloric acid solution is denoted as V_1. The acid value (AV) and AD were calculated according to Eq. (2), (3).

$$\mathrm{AV} = \frac{C_0 \times V_0 - C_1 \times V_1}{m} \quad (2)$$

$$\mathrm{AD}(\%) = M \times (AV_1 - AV_0) \times 100\% \quad (3)$$

where M is the molecular weight of grafting groups (85.08 g/L for *n*-valeryl, 153.21 g/mol for *n*- decanoyl and 211.32 g/mol for myristoyl), AV_0 and AV_1 are the AV value of the native and acylated anthocyanins, respectively.

The AD value of Na-An, Va-An, De-An and My-An, having done the calculation, were 0 %, 6.43 %, 7.56 % and 8.38 %, respectively.

2.5. Determination of octanol–water partition coefficien of the native and acylated blueberry anthocyanins

The lipid solubility of the acylated anthocyanins was characterised by octanol–water partition coefficient (KOW), which was measured as follows: 100 mL *n*-octyl alcohol was mixed with 300 mL ultra-pure water, stirred at a constant temperature for 24 h, and stored separately after standing for layering. 0.01 g of anthocyanins was dissolved in 5 mL saturated *n*-octyl alcohol and its absorbance at 513 nm was determined, denoted as A_0. Then 5 mL water saturated with *n*-octanol was added to the anthocyanin *n*-octanol solution, which was shaken for 1 h and centrifuged at 3000 RPM for 10 min. The upper *n*-octanol was taken and its absorbance at 513 nm was determined, denoted as A_1. The KOW value was expressed in terms as Log *P*, according to Eq. (4).

$$LogP = Log\frac{A_1}{A_0 - A_1} \quad (4)$$

2.6. Determination of the antioxidation activity of the native and acylated blueberry anthocyanins in vitro

The antioxidation activity of the native the acylated blueberry anthocyanins were measured in DPPH clearance and inhibition ratio in β-carotene bleaching assays, which were analysis according to previous study (Liu et al., 2021; Wang, Fei, Zhou, & Hong, 2021; Zhang, Zheng, Huang, & Fei, 2020).

2.6.1. Determination of DPPH clearance

5 mL DPPH solution was placed in a 7 mL centrifuge tube and its

absorbance at 513 nm was determined, denoted as A_0. Add 100 μL of anthocyanin solution to DPPH solution, mix well and place in dark environment. After 30 min, the absorbance of the above solution at 513 nm was determined, denoted as A_1. The DPPH clearance of the anthocyanins was calculated as Eq. (5):

$$DPPH\ clearance\% = \frac{A_0 - A_1}{A_0} \times 100 \quad (5)$$

2.6.2. Determination of inhibition ratio in β-carotene bleaching assay

Place 10 mL chloroform solution containing β-carotene (1 mg/mL) in a pear-shaped flask, add 400 μL linoleic acid and 4 mL tand80, mix well. The pear-shaped bottle was placed at 40 ℃ for evaporation to remove chloroform. Then, 100 mL distilled water is added to the above mixture and stirred evenly to form an emulsion. Take 10 mL emulsion, constant volume with water to 100 mL, mix evenly and get emulsified diluent.

In the experimental group, 4.8 mL emulsified diluent was added into a 7 mL centrifuge tube, 0.2 mL anthocyanin solution was added, and its absorbance at 470 nm was determined after homogenization, denoted as A_2. Another emulsified diluent was taken as the control group, 0.2 mL 30 % ethanol was added, and its absorbance at 470 nm was denoted as A_1.The control group and the experimental group were heated in an environment of 50 ℃. Two hours later, the absorbance of the emulsified diluent at 470 nm was determined. The absorbance of the control group was recorded as A_3, and that of the experimental group as A_4.

The inhibition ratio (Y) in β-carotene bleaching assay was calculated using Eq. (6):

$$Y = \left(1 - \frac{A_2 - A_4}{A_1 - A_3}\right) \times 100\% \quad (6)$$

2.7. Determination of the antioxidation activity of the native and acylated blueberry anthocyanins in C. elegans

2.7.1. Contemporaneous treatment of C. elegans

C. elegans was cultured in NGM medium until oviposition. Then, the medium was washed with M9 buffer to obtain the worms and their eggs. Next, 0.5 mL of sodium hypochlorite and 0.5 mL of sodium hydroxide (5 mol/L) were added to 4 mL of the above washing solution. After mixing and standing for 6 min, the supernatant was removed by centrifugation to obtain worm eggs. Afterword, wash the eggs 2–3 times with M9 buffer. Finally, the worm eggs were cultured on NGM medium with *E. coli* OP50 as food source for 48 h to L4 stage.

2.7.2. Determination of the MDA content and SOD activity

100 μL FUdR (50 mmol/L) and blueberry anthocyanin (20 g/L) mixed aqueous solution were added to above medium plate which containing worms and then cultured at 20℃. 5 days later, the worms were isolated and placed on a new NGM medium which containing *E. coli* OP50. Next, 100 μL of anthracite solution (10 mmol/L) was added to induce oxidative stress. After 24 h, the worms were picked out and cleaned 2–3 times with M9 buffer solution. Finally, the levels of MDA and SOD were determined using corresponding kits. The MDA content was measured through thiobarbituric acid assay and the SOD activity was determined by nitroblue tetrazolium assay.

2.8. Reaction mechanism analysis based on density functional theory (DFT)

In this paper, b3LYP method in Gaussian03 program package was used for all the calculations based on density functional theory. First, the molecular geometry was optimized in the 6-31G(d) module. The frequency calculations are performed to confirm the structures as minimum points in energy for all geometries. Then the energy calculation is performed on the module 6–311 + g(d, p). The temperature was set at 323 K, the solvent was set at tetrahydrofuran, and the frequency correction factor was 0.9804 (Lu & Chen, 2012).

2.9. Statistical analysis

Each experiment is made in triplicate, and the results are based on the average ± standard deviation. Statistical analyses were performed using SPSS 16.0. One-way ANOVA and independent sample *t*-test were conducted to compare the differences, which were considered statistically significant when $p < 0.05$. Origin 2021 is used for mapping and Excel for data analysis.

3. Results and discussion

3.1. Structural characterization

3.1.1. UV–vis and FTIR analysis

Fig. 1 show the UV–vis (a, b) and FTIR (c, d) spectra of the native and acylated blueberry anthocyanins. There are two characteristic peaks of anthocyanins in UV–vis spectra, locating at 500–540 nm (visible region) and 260–290 nm (ultraviolet region) respectively. Harborne et al (Harborne, 1958, 1986) reported that the acylated anthocyanins had a characteristic absorption band at 290–340 nm, assigning to the acyl group. As seen in Fig. 1 (a), compared to that of Na-An, the peak at 279.6 nm shifted to a lower wavelength at 267.8 nm, and a new absorption peak appeared at 291.8 nm. Obviously, the phenomenon was caused by the grafting of the fatty acids on the blueberry anthocyanins. In addition, the maximum absorption wavelength of the anthocyanins was found to be red shifted in Fig. 1(b) after acylating with all the three fatty acids, which also attributed to the introducing of the fatty acids. Moreover, a pronounced shoulder peak can be observed in the 440–460 nm region in Fig. 1(b), which indicated the position of glycosidic substitution is at C_3 position (Harborne, 1958, 1986), consistent with the previous literature.

The changes of anthocyanin molecular groups after acylation were displayed in Fig. 1(c, d). It can be easily observed that a broad absorption band located at ~ 3402 cm^{-1}, which was assigned to the stretching vibration of –OH and hydrogen bonds. It can be clearly seen that the peak at ~ 3402 cm^{-1} of the anthocyanins got narrow and sharp after grafting with the fatty acids. A reasonable explanation is that the hydrophobic molecule chains of the fatty acids were introduced to the blueberry anthocyanins and then broken the association between hydrogen bonds. The stronger the association between hydroxyl groups, the more hydrogen bonds, and the wider the absorption peak. The characteristic peak at ~ 1640 cm^{-1} was assigned to the vibrations of the benzene ring. The band at ~ 2924 cm^{-1} and 1441 cm^{-1} were caused by the stretching vibration and flexural vibration of $–CH_3$ and $–CH_2$, which got obviously stronger after grafting reaction (Cai et al., 2020; Zeng et al., 2021). Without doubt, the enhancement was due to the involving of the fatty acids, which contained abundant $–CH_3$ and $–CH_2$ groups. The peak at ~ 1726 cm^{-1} and the two peaks at ~ 1214 cm^{-1} and ~ 1149 cm^{-1} corresponding to the stretching vibration of C═O and C—O, respectively, of ester group got stronger after reacting with the fatty acids, which indicated that the fatty acids grafted onto the –OH of blueberry anthocyanins through acylation reaction. The anthocyanidins of the anthocyanins contain abundant phenolic hydroxyl groups while the glycosyls of that involve plentiful alcoholic hydroxyl groups. Generally speaking, the absorption of the C═O of chain-typed carboxylic ester located at ~ 1730 cm^{-1}, while that of C═C-COOR or Ar-COOR (Ar means aromatics) shifted to a lower wavenumber at ~ 1720 cm^{-1} due to the conjugation effect, and that of RCOO = C or RCOO-Ar shifted to higher wavenumber at ~ 1760 cm^{-1} due to the steric-hinerance effect. Moreover, a peak at 1585–1605 cm^{-1} attributed to benzene ring vibration was always observed in the FTIR spectrum of aromatic ester. As shown in Fig. 1 (d), it can be hardly observed both the peak at 1585–1605 cm^{-1} and the blueshift of the peak assigned to the stretching vibration of C═O. In view of above-mentioned reasons, it can be

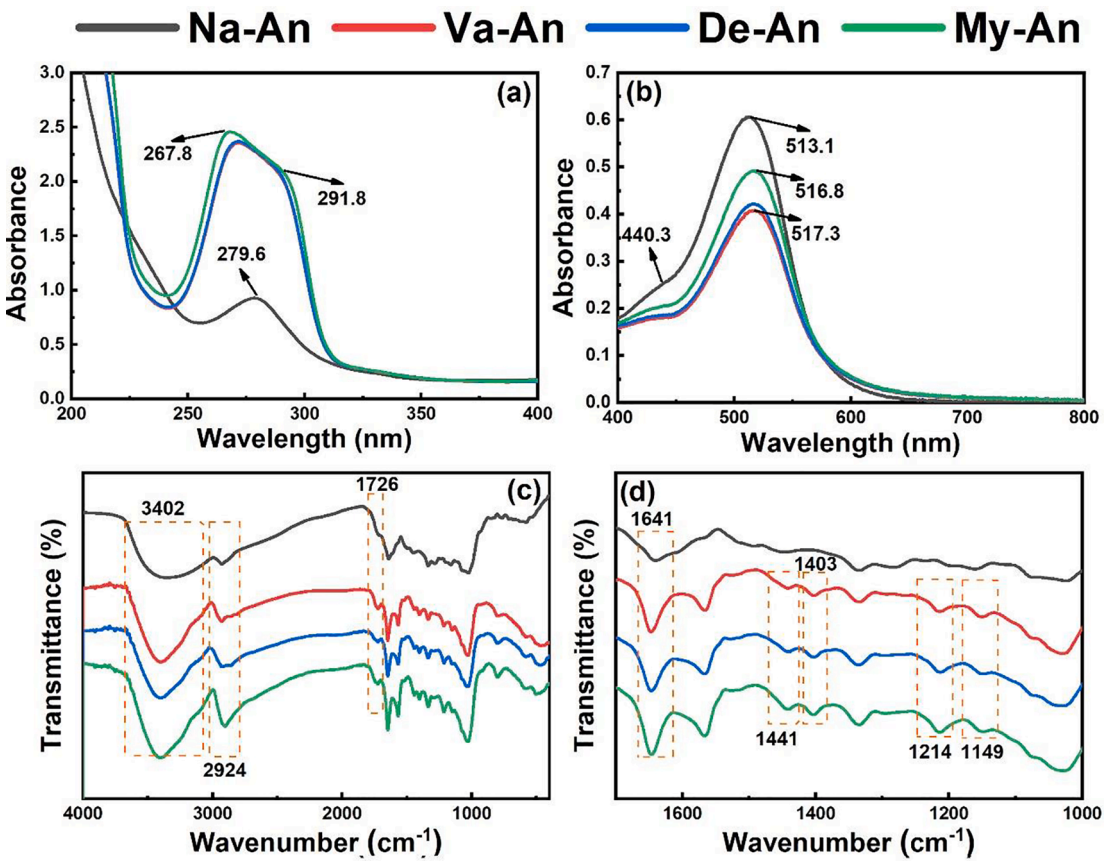

Fig. 1. UV–vis and FTIR spectra of the native and acylated blueberry anthocyanins.

deduced that the fatty acids mainly grafted onto the –OH of glycosyls of the blueberry anthocyanins.

3.1.2. XPS analysis

The electron binding energy of the carbon 1 s orbital and oxygen 1 s orbital in the native and acylated anthocyanins was characterised by using XPS and the results proceeded by overlapping peak resolving were presented in Fig. 2. It could be seen in Fig. 2(a) that the broad peak of C_{1s} of the native and acylated anthocyanins were consists of three single peaks, located at ~ 287.76 eV, ~286.08 eV and ~ 284.56 eV respectively, which indicated the three kinds chemical states of carbon in the anthocyanins. After grafting with fatty acids, the related intensity of the peak at ~ 284.56 eV decreased to a certain extent while that at ~ 286.08 were strengthen. Without doubt, the phenomenon was caused the introducing of fatty acids. In Fig. 2(b), the peak of C_{1s} of the native anthocyanins was made up of two single peaks, which was located at ~ 532.66 eV and ~ 531.26 eV. However, it could be hardly observed the peak at ~ 531.26 eV in the spectra of all the three the acylated anthocyanins. It is assumed that the grafting of fatty acids brought a large amount of carbon into the anthocyanins, which greatly reduced the oxygen content in the acylated anthocyanins and makes the differences between different chemical states of oxygen less obvious.

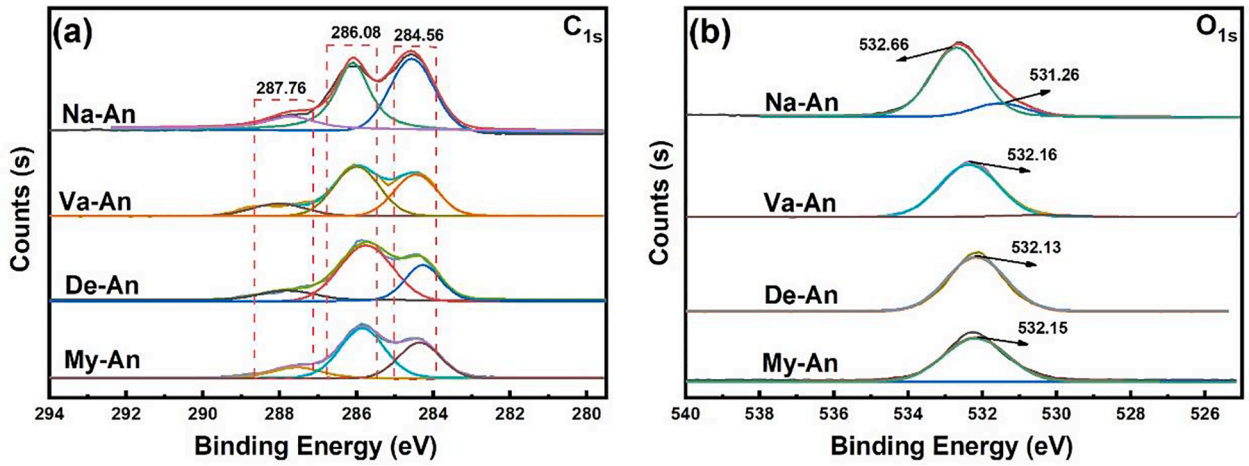

Fig. 2. XPS spectra of the native and acylated blueberry anthocyanins.

3.2. Reaction mechanism analysis based on DFT

3.2.1. Geometry of the optimized configurations and global properties of the investigated structures

This study is based on the nearing of the –COOH of the fatty acids from the active sides of cyanidin-3-O-glucoside (–OH). Based on B3LYP method at the 6–31 g(d) basis set, the geometric configurations of cyanidin-3-O-glucoside, valeric acid, decanoic acid and myristic acid were optimized and corresponding electrostatic potential distribution was calculated, which were presented in Fig. 3(a) (Lu & Chen, 2012).

On the basis of the optimization of geometric configuration, the global properties of 3-O-glucoside, valeric acid, decanoic acid and myristic acid were calculated and the results were shown in Fig. 3(b). According to frontier orbital theory, the highest occupied molecular orbital (HOMO) has the property of electron donor because of its relaxed binding on electrons. The lowest occupied molecular orbital (LOMO) has a strong affinity for electrons and is generally used as an electron acceptor. These two orbitals are most likely to interact with each other, and in general, the greater the absolute value of the difference between the two (E_{gap}), the stronger the reactivity (Huang et al., 2021). As shown in Fig. 3(b), the E_{gap} of valeric acid, decanoic acid and myristic acid were 7.7331, 7.6174 and 7.6117 eV, which meaned that the shorter the chain, the more reactive it was. This result was consistent with the result of AD values (presented in "part 2.3"). Vertical electron affinity (VEA) and vertical ionization potential (VIP) measured the accepting property (reduction power). These values presented in Fig. 3(b) also claimed that valerate has the lowest reduction power, which agreed with the result of AD values.

Besides, global hardness and global softness are also summarized in Fig. 3(b). In general, when the size of the molecule is constant, the smaller the hardness and the greater the softness of the molecule, the greater the reactivity of the molecule. In this case, myristic acid has the highest softness, but its chain is so long that the carboxyl group at the end of the chain is not easily accessible to the hydroxyl group of the anthocyanin molecule.

3.2.2. Relevant parameters of reactive active sites

The above analysis shows that the shorter the fatty acid molecular chain is, the easier it is to graft to anthocyanin molecules, which is consistent with the experimental results of AD. On this basis, it was assumed that the carboxyl group on valeric acid reacted with the eight hydroxyl groups on the molecule of cyanidin-3-O-glucoside respectively, and then the bond length and NBO charge population of each hydroxyl group were calculated and presented in Fig. 4. It could be easily observed in that both the bond length and the NBO charge population of the 6-OH were the highest among the eight phenolic hydroxyl groups. In general, the longer the bond length and the higher the NBO charge population, the higher the reactivity of the phenolic hydroxyl group, indicating the highest reactivity of 6-OH among all the eight hydroxyl groups. Besides, it could be obtained by density functional calculation that the reaction activation energy (E_a) was the lowest (30.23 KJ/mol) when valeric acid grafted on the 6-OH of the cyanidin-3-O-glucoside, which was agreed with the analysis above.

Previous studies have shown that blueberry anthocyanins mainly contain 15 anthocyanins (Tian, Giusti, Stoner, & Schwartz, 2005)., which are formed by the binding of 3 monosaccharides (glucose, galactose and arabinose) on the C3 site of 5 anthocyanidins (Cy, Dp, Pt, Mv and Pn). According to density functional theory and the reactive active sites of cyanidin-3-O-glucoside, it could be inferred that the fatty acids might be grafted onto the 6-OH of glycosyls and galactosyl and the 5-OH of arabinoside in the anthocyanin molecules through esterification reactions (Yang, Kortesniemi, Ma, Zheng, & Yang, 2019; Yang,

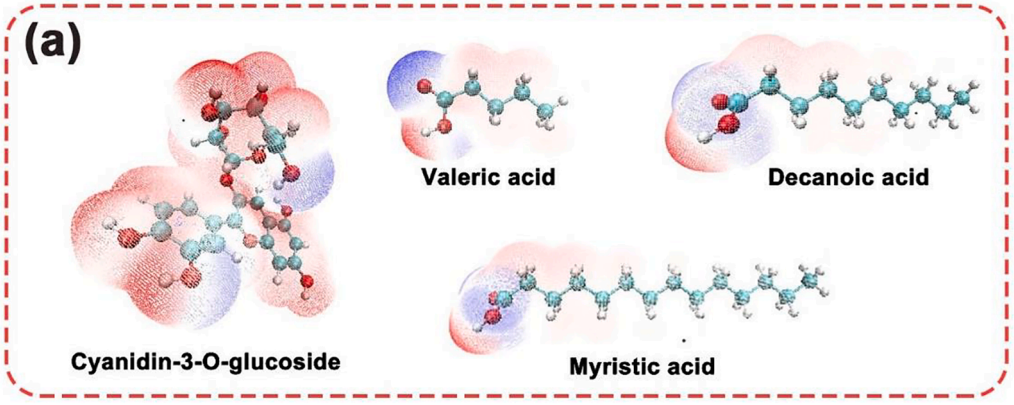

(b)

	Valeric acid	Decanoic acid	Myristic acid
E_{HOMO} (eV)	-7.4827	-7.2025	-7.2031
E_{LOMO} (eV)	0.2504	0.4148	0.4086
E_{gap} (eV)	7.7331	7.6174	7.6117
E_{VIP} (eV)	9.7930	9.2014	8.8885
E_{VEA} (eV)	-2.9155	-2.6657	-2.5567
Hardness (eV)	12.7085	11.8671	11.4452
Softness (eV)	0.0079	0.0084	0.0087

$E_{gap} = |E_{HOMO} - E_{LOMO}|$

Fig. 3. Geometry of the optimized configurations, electrostatic potential distribution (a) and global properties (b) of the investigated structures The darker the blue, the stronger the electrophilic ability; The darker the red, the stronger the electron loss. (For interpretation of the references to colour in this figure legend, the reader is referred to the web version of this article.)

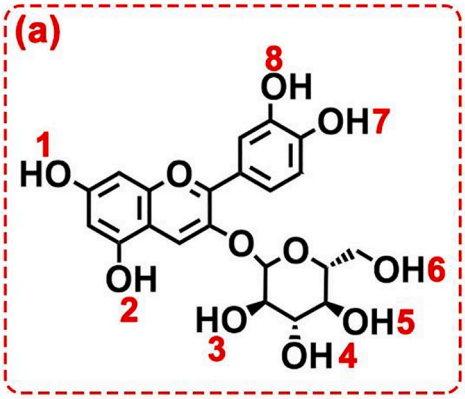

(b)

Reaction sites	Bond length (nm)	NBO Charge population	E_a (KJ/mol)
1	0.9737	0.500	117.20
2	0.9746	0.507	73.94
3	0.9719	0.519	138.69
4	0.9737	0.521	53.46
5	0.8723	0.536	91.30
6	0.9785	0.544	30.23
7	0.9746	0.530	107.32
8	0.9738	0.540	103.76

Fig. 4. Energy change of possible reactions.

Kortesniemi, Yang, & Zheng, 2018).

3.3. Lipid solubility of the native and acylated blueberry anthocyanins

The lipid solubility of the native and acylated blueberry anthocyanins was reflected by octanol–water partition coefficient (KOW) and the results were presented in Fig. 5 (Jin, Zhang, & Chai, 2022; Zhu, Su, Bao, Li, & Su, 2022). As seen in Fig. 5 (a), the *n*-octyl phase solution (located in the upper part of the centrifuge tube) was magenta and the aqueous phase solution (located in the lower half of the centrifuge tube) was dark red, when Na-An reached the distributive equilibrium between *n*-octyl and aqueous phase, which indicated the poor hydrophobicity of the native anthocyanins. While in the assays of Va-An, De-An and My-An, the *n*-octyl phase solution was dark red and the aqueous phase solution was pink. The KOW of the anthocyanins were measured based on the absorbance of the *n*-octyl phase solution and the aqueous phase solution and expressed in terms of Log *P*. As seen in Fig. 5 (b), the log *P* value of Na-An was −0.20 while the value of Va-An, De-An and My-An were 0.65, 0.66 and 0.72 respectively. The increased log *P* value after acylation reaction demonstrated the enhancement of fatty acids on the lipid solubility of the anthocyanins (Yang et al., 2018).

3.4. Antioxidation activity of the native and acylated blueberry anthocyanins in vitro and in C. elegans

The antioxidation activity of the native and acylated blueberry anthocyanins *in vitro* were evaluated in DPPH and β-carotene bleaching assays, and the results were presented in Fig. 6 (a) and (b). The DPPH clearance was 65.47 %, which decreased to 50.14 %, 52.83 % and 52.50 % respectively after grafting with *n*-valeric acid, *n*-decanoic acid and myristic acid. Apparently, the reduction of antioxidant groups in anthocyanins, which caused by the involving of the fatty acids was responsible for the decrease of the DPPH clearance. On one hand, some hydroxyl groups in anthocyanins bonded with fatty acids and then lost its ability to provide electrons and resist oxidation. On the other hand, the long aliphatic chains accumulated and winded around the surface of the anthocyanin molecules, thereby masking part of the antioxidant sites.

Besides, a different but interesting result can be observed in Fig. 6 (b). Compared with that of the native blueberry anthocyanins, the acylated blueberry anthocyanins showed stronger antioxidation in β-carotene bleaching assay. A possible explanation involved the different antioxidant mechanisms in DPPH clearance and β-carotene bleaching assay. In DPPH clearance assay, anthocyanins scavenged DPPH radicals by providing electrons, while in β-carotene bleaching assay, anthocyanins worked by inhibiting the oxidation of lipid. In detail, β-carotene, a polyene pigment, is easily oxidized by the peroxides produced by the oxidation of linoleic acid and then discolored. In the β-carotene emulsion, the anthocyanidins and glycosyls in the acylated anthocyanins were pulled toward the aqueous phase, and the fatty acid chains were pulled toward the oil phase (linoleic acid), thus the masked antioxidant active sites in the anthocyanin molecules are re-exposed. Meanwhile, the linoleic acid was coated with saturated fatty acids, which were less likely to oxidized to produce free radicals (Ossman, Fabre, & Trouillas, 2016). As a result, the acylated anthocyanins showed slightly higher inhibition ratio in β-carotene bleaching assay than that of the native anthocyanins. Of course, the impurities, including reducing sugars, ascorbic acid, organic acids, proteins, purines, sucrose et al., existed in the native and modified anthocyanins might interfere with the experimental results (Grobelna et al., 2019a, 2019b; Kalisz & Kieliszek, 2021; Kalisz et al., 2020). However, considering the super free radical scavenging ability of anthocyanins and their content in native

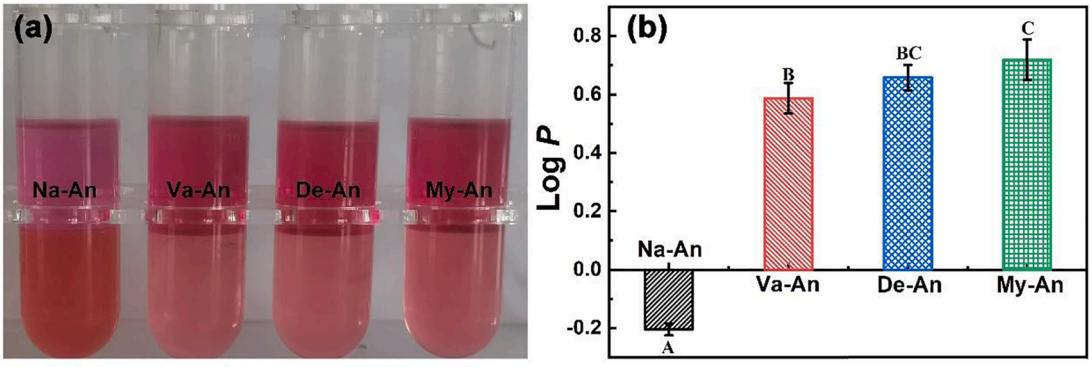

Fig. 5. KOW of the native and acylated blueberry anthocyanins Data represent mean ± standard deviation (n = 3); Different capital letters indicate statistical significance at $p < 0.05$.

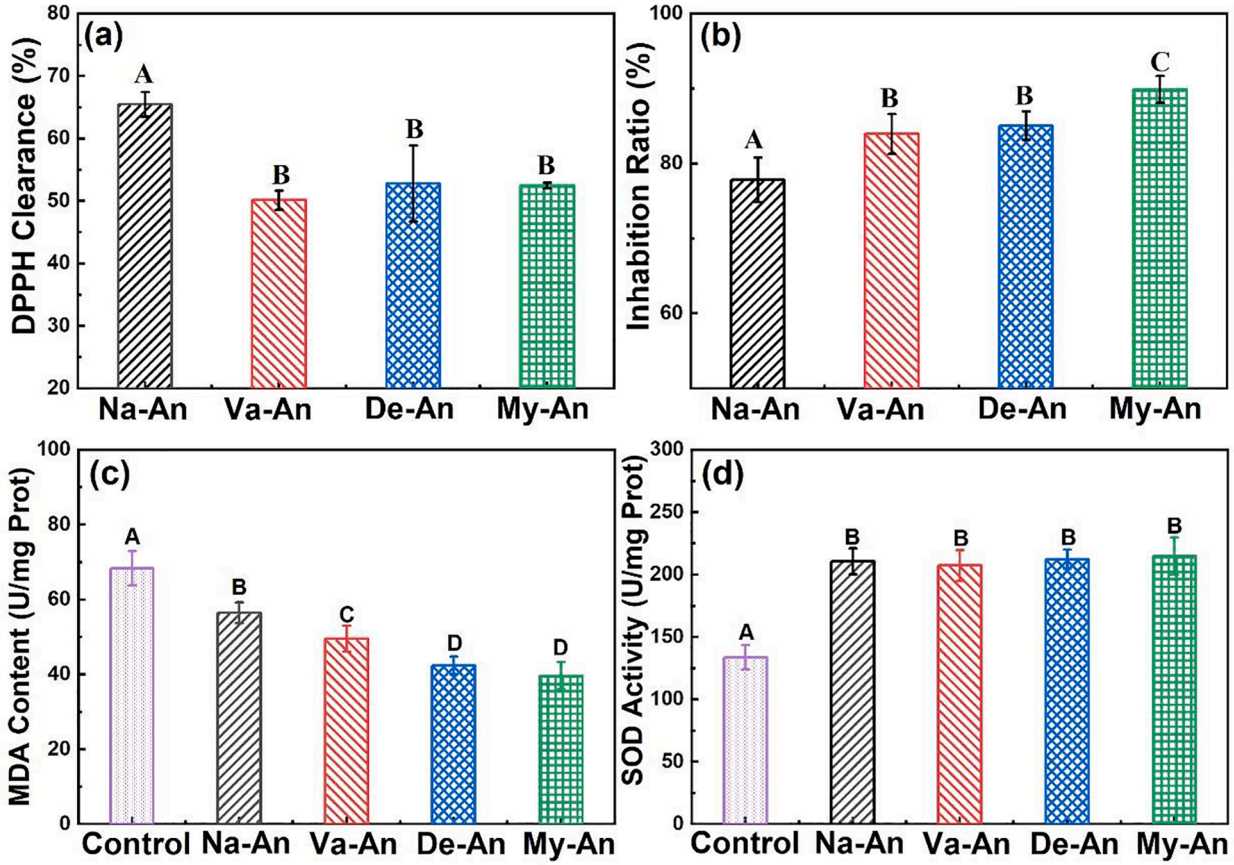

Fig. 6. Antioxidation activity of the native and acylated blueberry anthocyanins DPPH clearance (a) and inhibition ratio in β-carotene bleaching assay (b) *in vitro*; MDA content (c) and SOD activity (d) in *C. elegans* Data represent mean ± standard deviation (n = 3); Different capital letters indicate statistical significance at $p < 0.05$.

anthocyanins as high as 786.9 mg/g, together with some previous research results (Yang et al., 2019; Yang et al., 2018), it believed that the above inference is reasonable.

In addition to the antioxidant activity *in vitro*, the antioxidant activity of anthocyanins *in vivo* was characterized by MDA content and SOD activities by using *C. elegans* as a model organism. MDA is one of the most important products of lipid peroxidation in organism, so its content is an important parameter reflecting the potential antioxidant capacity of an organism (Gu et al., 2021; Ji et al., 2022). As seen in Fig. 6(a), it's clearly that the addition of the blueberry anthocyanins significantly reduced MDA content in *C. elegans*, indicating the inhibitory effect on lipid oxidation of the blueberry anthocyanins, and the effect of the acylated anthocyanins was stronger than that of the native anthocyanins. This might be due to the increased lipid solubility of anthocyanins caused by the introduction of fatty acids, which was in consistent with the results in the β-carotene bleaching experiment. Moreover, the activity of SOD, which is one of the most important antioxidant enzymes in living organisms, in the *C. elegans* was also measured and presented in Fig. 6(b). It could be seen from the figure that all the native and acylated anthocyanins could effectively inhibit the reduction of SOD activity in *C. elegans* induced by oxidative damage.

4. Conclusion

To improve the hydrophobicity of anthocyanins and expand their application in high-fat foods, in this study, fatty acids with high lipophilic properties, including *n*-valeric acid, *n*-decanoic acid and myristic acid, were grafted onto blueberry anthocyanins in this study, and the impact of the fatty acid side chains on the the anthocyanins were explored from several aspects. The results of UV–vis analysis and XPS analysis demonstrated that the three fatty acids were indeed grafted onto anthocyanin molecules through esterification reaction. FTIR analysis and DFT analysis further indicated that the shorter the chain of fatty acids, the more reactive they are, and the three fatty acids mainly grafted on the 6-OH of glycosyls and galactosyl and the 5-OH of arabinoside in the anthocyanins.

Then the hydrophobicity of the native and acylated blueberry anthocyanins were measured and expressed by the KOW. The value increased from −0.20 (Na-An) to 0.65 (Va-An), 0.66 (De-An) and 0.72 (My-An), which indicated that the fatty acid side chains greatly improved the hydrophobicity of the blue anthocyanins. Besides, the effects of the grafting of the fatty acids on the antioxidation activities of the anthocyanins were evaluated *in vitro* and in *vivo*. In *vitro* antioxidant experiments, the DPPH free radical scavenging rate of acylated anthocyanins was significantly lower than that of native blueberry anthocyanins, which may be caused by the covering of phenolic hydroxyl groups on anthocyanins. However, the inhibition ratio of acylated anthocyanins in *β*-carrot bleaching was higher than that of native anthocyanins. This might be due to the fact that acylated anthocyanins are more lipid soluble and thus more likely to inhibit oleic acid oxidation in the emulsion. In *C. elegans* assay, all the acylated anthocyanins and native anthocyanins could effectively increase SOD activity. In addition, acylated anthocyanins showed stronger inhibition of MDA generation than natural anthocyanins, which might be also caused by the improvement of anthocyanins lipid solubility due to the introduction of fatty acids.

CRediT authorship contribution statement

Pengkai Wang: Investigation, Data curation, Formal analysis, Writing – review & editing. **Jingna Liu:** Writing – original draft, Formal analysis. **Yuanhong Zhuang:** Data curation, Investigation. **Peng Fei:** Supervision, Project administration, Funding acquisition, Formal analysis, Writing – review & editing.

Declaration of Competing Interest

The authors declare that they have no known competing financial interests or personal relationships that could have appeared to influence the work reported in this paper.

Acknowledgement

The authors gratefully acknowledge the GuangDong Basic and Applied Basic Research Foundation (2021A1515110385), program for scientific research start-up funds of Guangdong Ocean University (060302042105) and Natural Science Foundation of Fujian Province of China (2021J01997, 2022J01905 and 2022J01909). In addition, the authors would like to thank Liquan Yan from Shiyanjia Lab (www.shiyanjia.com) for the XPS analysis.

References

Cai, J., Zeng, F., Zheng, S., Huang, X., Zhang, J., Zhang, P., & Fei, P. (2020). Preparation of Lipid-Soluble Bilberry Anthocyanins through Acylation with Cinnamic Acids and their Antioxidation Activities. *Journal of Agriculture and Food Chemistry, 68*(28), 7467–7473. https://doi.org/10.1021/acs.jafc.0c01912

Chandra Singh, M., Kelso, C., Price, W. E., & Probst, Y. (2020). Validated liquid chromatography separation methods for identification and quantification of anthocyanins in fruit and vegetables: A systematic review. *Food Research International, 138*, Article 109754. https://doi.org/10.1016/j.foodres.2020.109754

Chen, K., Wei, X., Kortesniemi, M., Pariyani, R., Zhang, Y., & Yang, B. (2022). Effects of acylated and nonacylated anthocyanins extracts on gut metabolites and microbiota in diabetic Zucker rats: A metabolomic and metagenomic study. *Food Research International, 153*, Article 110978. https://doi.org/10.1016/j.foodres.2022.110978

Fei, P., Zeng, F., Zheng, S., Chen, Q., Hu, Y., & Cai, J. (2021). Acylation of blueberry anthocyanins with maleic acid: Improvement of the stability and its application potential in intelligent color indicator packing materials. *Dyes and Pigments, 184*, Article 108852. https://doi.org/10.1016/j.dyepig.2020.108852

Grobelna, A., Kalisz, S., & Kieliszek, M. (2019a). Effect of Processing Methods and Storage Time on the Content of Bioactive Compounds in Blue Honeysuckle Berry Purees. *Agronomy, 9*(12). https://doi.org/10.3390/agronomy9120860

Grobelna, A., Kalisz, S., & Kieliszek, M. (2019b). The Effect of the Addition of Blue Honeysuckle Berry Juice to Apple Juice on the Selected Quality Characteristics, Anthocyanin Stability, and Antioxidant Properties. *Biomolecules, 9*(11). https://doi.org/10.3390/biom9110744

Gu, J., Li, Q., Liu, J., Ye, Z., Feng, T., Wang, G., … Zhang, Y. (2021). Ultrasonic–assisted extraction of polysaccharides from Auricularia auricula and effects of its acid hydrolysate on the biological function of Caenorhabditis elegans. *International Journal of Biological Macromolecules, 167*, 423–433. https://doi.org/10.1016/j.ijbiomac.2020.11.160

Harborne, J. B. (1958). Spectral methods of characterizing anthocyanins. *The Biochemical Journal, 70*(1), 22–28. https://doi.org/10.1042/BJ0700022

Harborne, J. B. (1986). The natural distribution in angiosperms of anthocyanins acylated with aliphatic dicarboxylic acids. *Phytochemistry, 25*(8), 1887–1894. https://doi.org/10.1016/S0031-9422(00)81168-1

He, J., & Giusti, M. M. (2010). Anthocyanins: Natural Colorants with Health-Promoting Properties. *Annual Review of Food Science and Technology, 1*(1), 163–187. https://doi.org/10.1146/ANNUREV.FOOD.080708.100754

Huang, B., Zhang, Z., Ding, N., Wang, B., Zhang, G., & Fei, P. (2021). Investigation of the pectin grafting with gallic acid and propyl gallate and their antioxidant activities, antibacterial activities and fresh keeping performance. *International Journal of Biological Macromolecules, 190*, 343–350. https://doi.org/10.1016/j.ijbiomac.2021.08.219

Ji, P., Li, H., Jin, Y., Peng, Y., Zhao, L., & Wang, X. (2022). *C. elegans* as an in vivo model system for the phenotypic drug discovery for treating paraquat poisoning. *PeerJ, 10*, e12866.

Jin, H., Zhang, C., & Chai, X. (2022). Determination of methanol partition coefficient in octanol/water system by a three-phase ratio variation headspace gas chromatographic method. *Journal of Chromatography A, 1665*, Article 462825. https://doi.org/10.1016/j.chroma.2022.462825

José Aliaño González, M., Carrera, C., Barbero, G. F., & Palma, M. (2022). A comparison study between ultrasound–assisted and enzyme–assisted extraction of anthocyanins from blackcurrant (Ribes nigrum L.). *Food Chemistry: X, 13*. https://doi.org/10.1016/j.fochx.2021.100192

Kalisz, S., & Kieliszek, M. (2021). Influence of storage conditions on selected quality characteristics of blue honeysuckle berry juice. *Agrochimica -Pisa-, 66*, 25–37. https://doi.org/10.12871/00021857202112

Kalisz, S., Oszmiański, J., Kolniak-Ostek, J., Grobelna, A., Kieliszek, M., & Cendrowski, A. (2020). Effect of a variety of polyphenols compounds and antioxidant properties of rhubarb (Rheum rhabarbarum). *LWT-Food Science and Technology, 118*, Article 108775. https://doi.org/10.1016/j.lwt.2019.108775

Liu, J., Wang, T., Huang, B., Zhuang, Y., Hu, Y., & Fei, P. (2021). Pectin modified with phenolic acids: Evaluation of their emulsification properties, antioxidation activities, and antibacterial activities. *International Journal of Biological Macromolecules, 174*, 485–493. https://doi.org/10.1016/j.ijbiomac.2021.01.190

Liu, J., Zhuang, Y., Hu, Y., Xue, S., Li, H., Chen, L., & Fei, P. (2020). Improving the color stability and antioxidation activity of blueberry anthocyanins by enzymatic acylation with p-coumaric acid and caffeic acid. *LWT-Food Science and Technology, 130*, Article 109673. https://doi.org/10.1016/j.lwt.2020.109673

Lu, T., & Chen, F. (2012). Quantitative analysis of molecular surface based on improved Marching Tetrahedra algorithm. *Journal of Molecular Graphics and Modelling, 38*, 314–323. https://doi.org/10.1016/j.jmgm.2012.07.004

Lu, T., & Chen, F. W. (2012). Multiwfn: A multifunctional wavefunction analyzer. *Journal of Computational Chemistry, 33*(5), 580–592. https://doi.org/10.1002/jcc.22885

Oliveira Filho, J. G. D., Braga, A. R. C., Oliveira, B. R. D., Gomes, F. P., Moreira, V. L., Pereira, V. A. C., & Egea, M. B. (2021). The potential of anthocyanins in smart, active, and bioactive eco-friendly polymer-based films: A review. *Food Research International, 142*, Article 110202. https://doi.org/10.1016/j.foodres.2021.110202

Ossman, T., Fabre, G., & Trouillas, P. (2016). Interaction of wine anthocyanin derivatives with lipid bilayer membranes. *Computational and Theoretical Chemistry, 1077*, 80–86. https://doi.org/10.1016/j.comptc.2015.10.034

Pinheiro, E. S. R., Silva, I. M. D. A., Gonzaga, L. V., Amante, E. R., Teófilo, R. F., Ferreira, M. M. C., & Amboni, R. D. M. C. (2008). Optimization of extraction of high-ester pectin from passion fruit peel (Passiflora edulis flavicarpa) with citric acid by using response surface methodology. *Bioresource Technology, 99*(13), 5561–5566. https://doi.org/10.1016/j.biortech.2007.10.058

Stoica, F., Condurache, N. N., Aprodu, I., Andronoiu, D. G., Enachi, E., Stănciuc, N., … Râpeanu, G. (2022). Value-added salad dressing enriched with red onion skin anthocyanins entrapped in different biopolymers. *Food Chemistry: X, 15*, Article 100374. https://doi.org/10.1016/j.fochx.2022.100374

Tian, Q., Giusti, M. M., Stoner, G. D., & Schwartz, S. J. (2005). Screening for anthocyanins using high-performance liquid chromatography coupled to electrospray ionization tandem mass spectrometry with precursor-ion analysis, product-ion analysis, common-neutral-loss analysis, and selected reaction monitoring. *Journal of Chromatography A, 1091*(1), 72–82. https://doi.org/10.1016/J.CHROMA.2005.07.036

Wang, P., Fei, P., Zhou, C., & Hong, P. (2021). Preparation of acylated pectins with phenolic acids through lipase-catalyzed reaction and evaluation of their preservation performance. *LWT-Food Science and Technology, 147*, Article 111615. https://doi.org/10.1016/j.lwt.2021.111615

Yang, W., Kortesniemi, M., Ma, X., Zheng, J., & Yang, B. (2019). Enzymatic acylation of blackcurrant (Ribes nigrum) anthocyanins and evaluation of lipophilic properties and antioxidant capacity of derivatives. *Food Chemistry, 281*, 189–196. https://doi.org/10.1016/j.foodchem.2018.12.111

Yang, W., Kortesniemi, M., Yang, B., & Zheng, J. (2018). Enzymatic Acylation of Anthocyanins Isolated from Alpine Bearberry (Arctostaphylos alpina) and Lipophilic Properties, Thermostability, and Antioxidant Capacity of the Derivatives. *Journal of Agriculture and Food Chemistry, 66*(11), 2909–2916. https://doi.org/10.1021/acs.jafc.7b05924

Zeng, F., Zeng, H., Ye, Y., Zheng, S., Zhuang, Y., Liu, J., & Fei, P. (2021). Preparation of acylated blueberry anthocyanins through an enzymatic method in an aqueous/organic phase: Effects on their colour stability and pH-response characteristics. *Food & Function, 12*(15), 6821–6829. https://doi.org/10.1039/d1fo00400j

Zeng, P., Chen, X., Qin, Y., Zhang, Y., Wang, X., Wang, J., … Zhang, Y. (2019). Preparation and characterization of a novel colorimetric indicator film based on gelatin/polyvinyl alcohol incorporating mulberry anthocyanin extracts for monitoring fish freshness. *Food Research International, 126*, Article 108604. https://doi.org/10.1016/j.foodres.2019.108604

Zhang, G., Zheng, C., Huang, B., & Fei, P. (2020). Preparation of acylated pectin with gallic acid through enzymatic method and their emulsifying properties, antioxidation activities and antibacterial activities. *International Journal of Biological Macromolecules, 165*, 198–204. https://doi.org/10.1016/j.ijbiomac.2020.09.195

Zhao, C., Yu, Y., Chen, Z., Wen, G., Wei, F., Zheng, Q., … Xiao, X. (2017). Stability-increasing effects of anthocyanin glycosyl acylation. *Food Chemistry, 214*, 119–128. https://doi.org/10.1016/j.foodchem.2016.07.073

Zhu, M., Su, H., Bao, Y., Li, J., & Su, G. (2022). Experimental determination of octanol-water partition coefficient (KOW) of 39 liquid crystal monomers (LCMs) by use of the shake-flask method. *Chemosphere, 287*, Article 132407. https://doi.org/10.1016/j.chemosphere.2021.132407